

1

Xolotl: An Intuitive and Approachable Neuron and Network Simulator for Research and Teaching

Srinivas Gorur-Shandilya^{1*†}, Alec Hoyland^{1†}, and Eve Marder¹

¹ *Volen National Center for Complex Systems and Biology Department
Brandeis University
Waltham, MA 02453
USA*

† *These authors have equally contributed to this article.*

Correspondence*:

Srinivas Gorur-Shandilya

Volen National Center for Complex Systems, Brandeis University, Waltham MA
02454

srinivasgs@brandeis.edu

An Intuitive Neuronal Simulator

2 ABSTRACT

3 Conductance-based models of neurons are used extensively in computational neuroscience.
4 Working with these models can be challenging due to their high dimensionality and large number
5 of parameters. Here, we present a neuron and network simulator built on a novel automatic type
6 system that binds object-oriented code written in C++ to objects in MATLAB. Our approach builds
7 on the tradition of uniting the speed of languages like C++ with the ease-of-use and feature-set
8 of scientific programming languages like MATLAB. Xolotl allows for the creation and manipula-
9 tion of hierarchical models with components that are named and searchable, permitting intuitive
10 high-level programmatic control over all parts of the model. The simulator's architecture allows
11 for the interactive manipulation of any parameter in any model, and for visualizing the effects
12 of changing that parameter immediately. Xolotl is fully featured with hundreds of ion channel
13 models from the electrophysiological literature, and can be extended to include arbitrary con-
14 ductances, synapses, and mechanisms. Several core features like bookmarking of parameters
15 and automatic hashing of source code facilitate reproducible and auditable research. Its ease
16 of use and rich visualization capabilities make it an attractive option in teaching environments.
17 Finally, xolotl is written in a modular fashion, includes detailed tutorials and worked examples,
18 and is freely available at <https://github.com/sg-s/xolotl>, enabling seamless integration into the
19 workflows of other researchers.

20 **Keywords:** code:MATLAB, code:C++, conductance-based, software, Hodgkin-Huxley

1 INTRODUCTION

21 Nervous systems process and transmit information using electrically excitable membranes. Conductance-
22 based models are a powerful biophysical simplification of an electrically excitable compartment in a

23 neuron (Hodgkin and Huxley 1952a). Studies based on the Hodgkin-Huxley formalism now contribute
24 significantly to mainstream research in some circuits (Marder and Abbott 1995; Prinz 2010; Prinz 2006).
25 These models provide an approachable framework for understanding many salient principles of electro-
26 physiology, since they explicitly model cell membranes and ion channels as electrical components in a
27 circuit. However, several challenges remain in working with biophysically-detailed conductance-based
28 neuron models. First, these models can be high-dimensional with many nonlinear differential equations,
29 each with several parameters. Second, many or all equations in these models can be strongly coupled
30 through dynamical variables like the membrane potential. In multi-compartment models of spatially ex-
31 tended neurons, membrane potentials in every compartment can be different, and are coupled to each
32 other. Finally, the choice of programming language used to implement the model imposes tradeoffs in
33 designing and using neuron and network simulators: simulators written in languages like C++ or FOR-
34 TRAN can integrate equations quickly, but often lack the ease-of-use and interoperability of those written
35 in scientific programming languages like Python, Julia, or MATLAB (Mathworks).

36 Two major approaches have dominated the design of neuron simulators. One approach is to write the
37 simulator in a fast compiled language like C and allow for the construction and simulation of neuron
38 models using object-oriented paradigms. This approach has been implemented in NEURON (Hines and
39 Carnevale 1997). Simulators designed in this way tend to perform fast computations with little overhead,
40 but suffer from a steep learning curve. Wrapping these simulators in a more approachable language like
41 Python or using graphical user interfaces (GUIs) mitigates these drawbacks (Hines, Davison, and Muller
42 2009; Gratiy et al. 2018) at the cost of obfuscating the underlying algorithms and parameters (Brette
43 et al. 2007; Hines, Davison, and Muller 2009). In contrast, simulators designed from the ground up in
44 popular scientific computing languages can be easier to use and benefit from interoperability with other
45 commonly-used tools. Simulators like DynaSim (Sherfey et al. 2018), ANNarchy (Vitay, Dinkelbach,
46 and Hamker 2015), BRIAN (Stimberg et al. 2013), morphforge (Hull and Willshaw 2014), and PyNN
47 (Davison et al. 2009) allow the user to specify models with strings of equations or components that are
48 constructed using a special syntax, that can then be translated into a faster implementation language
49 such as C or C++ (Stimberg et al. 2014a). This approach permits considerable flexibility for simulating
50 systems of differential equations. Because models need to be translated between the two languages, the
51 hierarchical nature of neuron models is not naturally encapsulated by these tools, and the syntax can
52 be verbose. Neither approach facilitates the creation of tools that simultaneously maintain efficiency,
53 ease-of-use, and clarity.

54 To overcome these design limitations, we have developed a novel automatic type system, that we call
55 `cpplab`, which binds MATLAB code to classes specified in C++ header files. This architecture automat-
56 ically creates objects in MATLAB that represent the underlying object-oriented C++ code, allowing the
57 symbolic manipulation of C++ objects in the MATLAB interface. In this paper, we introduce `xolotl`, an
58 implementation of the `cpplab` system specialized in integrating conductance-based neuron and network
59 models. Models can be easily constructed from components of different types in a few lines of MATLAB
60 code using a hierarchical and intuitive syntax. Since models in the MATLAB workspace are automatically
61 linked to models in the C++ implementation, configuring these objects in MATLAB transparently config-
62 ures the underlying C++ objects. `Xolotl` comes packaged with hundreds of components that can be used
63 to assemble cells and networks; has built-in visualization functions to inspect voltage time traces and acti-
64 vation functions; and a GUI for real-time manipulation of model parameters. `Xolotl`'s ease of use makes it
65 an attractive option for pedagogical applications, rapid prototyping of models, and primary research use.
66 Our software aims to simplify the investigation of the dynamics of conductance-based network and neu-
67 ron models, facilitate collaborative modeling, and is intended to complement other tools being developed
68 in the computational neuroscience community.

2 DESIGN GOALS

69 Xolotl is designed to be easy-to-use and richly featured while being fast enough to use in everyday
70 research. Our focus was on designing an approachable simulator of conductance-based neurons and net-
71 works of these neurons; simulating arbitrary dynamical systems is therefore beyond the scope of this
72 software. Specifically, the software was designed to simulate models of the form

$$C_i \frac{dV_i}{dt} = - \sum_j I_j \quad (1)$$

73 where C_i and V_i are the capacitance and membrane potential of compartment i . Compartments can
74 represent whole neurons or parts of neurons. I_j is the current due to ion channel population j and is given
75 by

$$I_j = \bar{g}_j m_j^p h_j^q (V - E_j) A_i \quad (2)$$

76 Here, \bar{g}_j is the maximal conductance, and E_j is the reversal potential of the ion channel population j .
77 A_i is the surface area of compartment i that contains these ion channels. m_j and h_j are activation and
78 inactivation variables that change according to

$$\tau_m \frac{dm}{dt} = m_\infty - m \quad \text{and} \quad \tau_h \frac{dh}{dt} = h_\infty - h$$

79 Typically, τ_m , τ_h , m_∞ , and h_∞ are functions of the membrane potential V_i . The software uses integration
80 schemes that have been specifically developed to solve equations of this form (Dayan and Abbott 2001;
81 Hines 1984; Oh and French 2006), though other schemes can be used if desired.

82 This software is designed to be used from within MATLAB, a scientific programming language com-
83 mon amongst neuroscientists and engineers for pedagogy and research. Our goal was to make xolotl
84 completely usable entirely from within MATLAB. Models created using this simulator appear in the
85 MATLAB workspace as native objects, are thus fully scriptable, and are fully compatible with the large
86 library of toolboxes that MATLAB provides, allowing the software to be used as a component of other
87 packages and tools. All parameters of a model, and activation functions of any channel can be inspected
88 at any point. We designed several features of the simulator to be easily extensible: adding custom con-
89 ductances or synapse types is possible by calling functions that generate new C++ files on-the-fly. Finally,
90 xolotl is fully auditable by design, with several tools to verify model and parameter integrity and aid in
91 reproducibility.

2.1 FEATURES

92 *Object-oriented.* Xolotl is designed to mirror the nested and hierarchical structure of networks and neu-
93 rons. Biological neuronal networks are made up of neurons that are connected to each other with synapses.
94 Each of these neurons contains within it a set of conductances and synaptic currents that contribute to its
95 electrical behavior. Intracellular mechanisms can act within the cell, or parts of the cell, to modify and
96 regulate conductances, synapses, or other dynamic properties of the cell. Similarly, a xolotl model can
97 contain a set of compartments that can represent individual neurons. Each compartment can contain an
98 arbitrary set of conductances. Compartments, conductances and synapses can contain mechanisms that
99 can affect anything in the model. All objects in the xolotl model tree (compartments, conductances, etc.)
100 are bonafide MATLAB objects with their own type and properties. This object-oriented programming
101 paradigm naturally represents the hierarchical structure of biological networks that contain neurons that

102 contain populations of ion channels, and makes constructing, integrating, and thinking about these models
103 easier.

104 *A rich library of network components.* Xolotl comes packaged with hundreds of pre-existing components
105 (compartments, synapses, conductances, and mechanisms) that can be used as building blocks to construct
106 model neurons and networks. “Compartments” represent sections of membrane with a single membrane
107 potential, intracellular Calcium concentration, and set of constituent components; and can represent either
108 entire cells or parts of cells. Objects of type “conductance” represent populations of ion channels in a
109 compartment that produce transmembrane currents. “synapse” objects connect two compartments together
110 by introducing a current in the postsynaptic compartment that depends on the presynaptic compartment’s
111 membrane potential. Objects of type “mechanism” can represent any intracellular mechanism and can
112 read and modify any other component in the cell, and can run arbitrary dynamical systems within them.
113 Parameters of any of these objects can be easily inspected and modified at any time, either manually or
114 through a programmatic interface.

115 *Automatic type system.* To circumvent the tradeoff between high-performance but hard-to-use languages
116 like C++ and richly-featured but potentially slow languages like MATLAB, we constructed an automatic
117 type system that links object oriented code in C++ to object oriented code in MATLAB. This architecture
118 lets us construct the core of the simulator in C++, leveraging features of C++ like pointers that are not
119 readily available in MATLAB. A rudimentary way to make this C++ code useable in MATLAB would
120 be to re-write that code in MATLAB so that MATLAB objects can be bound to their C++ implemen-
121 tations. However, this approach is cumbersome and inefficient, and can introduce errors. Instead, our
122 automatic type system creates objects in MATLAB on-the-fly from C++ class specifications, obviating
123 the need to rewrite code in MATLAB while preserving a tight coupling between objects in the MATLAB
124 workspace and their C++ implementation. Crucially, this method makes developing new code much easier
125 and simplifies the task of constructing complex frameworks that span these two languages.

126 *Automatic hashing and compiling.* Because every model requires a compiled binary to run, a potential
127 stumbling block is the problem of unambiguously linking a model to a binary executable. Xolotl solves
128 this problem by hashing (Rivest 1992) the C++ header files of every component in the model recursively,
129 allowing a model, no matter how complex, to be compactly represented by a short alphanumeric identifier
130 (its “hash”). Compiled binaries are named using this hash, ensuring both that the correct binary is run
131 to integrate the model, and that compilation occurs only as needed. This powerful feature enables the
132 user experience to remain entirely within the MATLAB workspace, with compilation and selection of the
133 correct binary occurring silently in the background.

2.2 LIMITATIONS

134 Our focus on xolotl’s ease-of-use and speed imposed some limitations on its feature set.

135 *Limited to conductance-based models.* xolotl has been developed specifically for conductance-based
136 models. It does not currently support rate- or current-based models, or arbitrary dynamical systems.

137 *Limited numerical integration strategies.* Most components in the software are integrated using the expo-
138 nential Euler method, which has been used in integrating neuronal models (Oh and French 2006; Dayan
139 and Abbott 2001). However, it may be desirable to use other methods under certain conditions. It is
140 possible to introduce new components that implement other integration schemes, or to modify the inte-
141 gration schemes of existing components, but that requires writing new C++ code. Currently, xolotl can
142 only implement integration schemes with fixed step size.

143 *Inefficient tools for handling large networks.* xolotl was designed to work with small but complex net-
144 works and models, where every compartment and component is named, rather than numbered. It is

145 more therefore suited towards simulating small, heterogeneous networks rather than large, homoge-
146 nous networks. While the software can integrate large networks (> 1000 compartments), other tools
147 are presumably more suited to this task, offering more natural frameworks for dealing with a large num-
148 ber of identical units. Similarly, xolotl is not optimized to solve coupled ODEs on complex branched
149 morphologies, that other simulators like NEURON (Hines and Carnevale 1997) are specialized for.

150 *New mechanisms require new C++ code.* Adding new network components requires writing new C++
151 code. A new conductance in the Hodgkin-Huxley formalism (Hodgkin and Huxley 1952b; Hodgkin,
152 Huxley, and Katz 1952; Hodgkin and Huxley 1952a; Dayan and Abbott 2001) requires creating a new
153 C++ header file, though this is generally trivial. Implementing a new integration scheme or component
154 type requires much more in-depth knowledge of the underlying C++ core code.

3 USAGE EXAMPLES

155 In this section, we illustrate how xolotl can be used to generate, inspect, and simulate a variety of models.
156 These examples have been chosen to demonstrate various features of xolotl, and are intended to serve as
157 templates upon which researchers and educators can build.

3.1 SIMULATING A HODGKIN-HUXLEY MODEL

158 The axon of the giant squid contains a fast inactivating sodium conductance (NaV), a slower non-
159 inactivating potassium conductance (Kd), and a passive leak current (Leak). Seminal work by Hodgkin
160 and Huxley showed that depolarizations of the membrane could lead to an activation of the voltage-
161 sensitive NaV channels, which led to a run away depolarization that was terminated by the inactivation
162 of NaV channels and the activation of Kd channels that repolarized the membrane (Hodgkin and Huxley
163 1952b; Hodgkin, Huxley, and Katz 1952). As one of the simplest models of excitable neural membranes,
164 the Hodgkin-Huxley model often serves as the first model introduced in pedagogical literature (Dayan
165 and Abbott 2001; Sterratt 2011; Trappenberg 2010).

166 In this example, we demonstrate how to simulate the spiking activity of a Hodgkin-Huxley-like model,
167 and how the tools built into xolotl make it easy to set up and integrate the model and gain insight into the
168 underlying biophysical mechanisms. This simple model consists of a single electrical compartment with
169 three types of conductances (Figure 1A). This hierarchical organization of the neuron is mirrored in the
170 structure of the model in the simulator: an object of type “compartment” is used to represent the cell body,
171 and three objects of type “conductance” are used to model the three populations of ion channels (Figure
172 1B). These models of ion channels were obtained from (Liu et al. 1998) based on electrophysiological
173 recordings from the lobster stomatogastric ganglion (Turrigiano, LeMasson, and Marder 1995), and are
174 part of the simulator. The code to set up this model is terse, idiomatic, relies on no special markup, and
175 preserves the hierarchical nature of the model (Figure 1C).

176 Adding an injected current and calling the built-in `plot` function plots the time series of membrane
177 voltage. In the absence of injected current, the model is quiescent. When 0.2 nA is injected, the model
178 tonically spikes (Figure 1A-B). The `plot` function displays a voltage trace colored by the dominant
179 current (Figure 1A). Colors in the voltage trace indicate the strongest instantaneous inward current when
180 the voltage is increasing, and strongest instantaneous outward current when the voltage is decreasing.
181 This built-in feature reveals that the dominant current during the upswing of every action potential is
182 the sodium current, and the dominant current immediately after the peak of the action potential is the
183 potassium current, but that the leak current contributes to depolarization following an action potential.
184 This feature could be useful in quickly understanding the contributions of a number of ion channel types
185 in a complex voltage trace from a more complicated neuron model.

186 Integrating the model returns the voltage time series for every compartment:

```
187 V = x.integrate;
```

188 The model can be integrated for various amplitudes of injected current to determine its F-I (frequency
189 current) curve (Kispersky, Caplan, and Marder 2012). Figure 1E shows the F-I curve of this model,
190 obtained by repeated integration of the model. Finally, the built-in `show` function can plot activation
191 (m) and inactivation (h) curves and voltage-dependent timescales of any channel type in the simulator
192 (Figure 1D-G). These plots reveal that activation kinetics of the NaV channels are much faster than that
193 of the Kd channels (Figure 1F), which facilitates the transient depolarization in an action potential. In
194 summary, the simulator allows the user to construct and integrate this model in a few lines of code, and
195 provides rich visualization of the dynamics of the model.

3.2 PERFORMING A VOLTAGE CLAMP EXPERIMENT *IN-SILICO*

196 Voltage clamping is an experimental technique where a amplifier is configured to inject the appropri-
197 ate amount of current through a electrode to maintain the voltage of a cell at a desired value (Dayan
198 and Abbott 2001). Under this paradigm, the membrane voltage is “clamped” or fixed to a desired value,
199 permitting the study of voltage-dependent ion channels, since the sum of all currents through the popu-
200 lation of ion channels in the cell is equal and opposite to the current injected by the clamp (Figure 2A).
201 By combining voltage clamp with the use of pharmacological agents to block all channels but the one
202 of interest, the voltage-sensitivity of an ion channel population can be characterized (Cole and Moore
203 1960; Cole 1955; Hodgkin and Katz 1949; Hodgkin, Huxley, and Katz 1952; Hodgkin and Huxley 1952a;
204 Turrigiano, LeMasson, and Marder 1995).

205 Xolotl can reproduce such a voltage clamp experiment *in-silico*. Figure 2B illustrates how a simple
206 model with a single compartment and a single ion channel type can be set up and clamped to a desired
207 voltage. Integrating the model yields the current required to clamp the cell at that voltage. Here, we use a
208 delayed-rectifier potassium conductance (Liu et al. 1998) and simulate a voltage-clamp experiment whose
209 goal is to infer the activation function of this channel. First, the cell is clamped to a number of different
210 voltages (Fig. 2C) and the resultant clamp currents are measured by integrating the model (Fig. 2D). Since
211 the compartment is being voltage clamped, integrating the model returns the clamping current:

```
212 I_clamp = x.integrate;
```

213 By repeating the integration at a number of clamp voltages, we observe that the asymptotic clamp
214 currents depend on the clamp voltage in a nonlinear manner (Fig. 2E), since the open probabilities of
215 the channel are functions of the membrane voltage. Assuming the reversal potential is known, Eq. (2)
216 can be used to solve for the total conductance of the channel as a function of the clamp voltage (Fig.
217 2F). Finally, a sigmoid can be fit to the normalized conductance-voltage curves to obtain the activation
218 function of the ion channel population (Fig. 2G-H). Xolotl can therefore be used to describe graphically
219 the theoretical underpinnings of ion channel characterization through voltage clamp and can serve as an
220 effective pedagogical tool in computational neuroscience.

3.3 INTRACELLULAR MECHANISMS

221 So far, the models we described only considered the voltage dynamics of a cell (the solution to Eq. 1).
222 However, real neurons possess several dynamical features, arising from a variety of intracellular mecha-
223 nisms. Xolotl makes it possible to model and include arbitrary intracellular mechanisms. In xolotl, these
224 intracellular mechanisms are represented by the “mechanism” object, and can be bound to compartments,
225 conductances, and other object types.

226 A key intracellular mechanism is the cytosolic buffering of Calcium and its influx through voltage-
227 gated Calcium channels. Figure 3A shows a model of a single-compartment model with 8 populations
228 of ion channels (Liu et al. 1998). Without any explicit mechanism for Calcium influx or buffering, the
229 intracellular Calcium levels in this model do not change (Figure 3B) and the model tonically spikes (Figure

230 3C). Calcium buffering and influx can be modeled by a differential equation that increases intracellular
231 Calcium with the current through Calcium channels and relaxes back to a baseline value (Liu et al. 1998;
232 Prinz, Billimoria, and Marder 2003; Dayan and Abbott 2001) (Figure 3D). This mechanism exists in the
233 xolotl library as `CalciumMech1` and can be added to the model using a simple `add` statement (Figure
234 3E). The intracellular Calcium in the model now oscillates periodically (Figure 3F), synchronized to bursts
235 in action potentials in this cell (Figure 3G).

236 Neurons can regulate their electrical activity by controlling the spectrum of ion channels they express
237 (MacLean et al. 2003; Turrigiano, LeMasson, and Marder 1995; Schulz, Goaillard, and Marder 2006).
238 Here, we will show how xolotl can be used to represent a recently proposed model of a homeostatic
239 feedback system that controls the transcription rates of ion channels with the integral of an error signal
240 derived from the intracellular Calcium concentration (O’Leary et al. 2013; O’Leary et al. 2014) (Figure
241 3H). Since this mechanism affects each ion channel population individually, an object corresponding
242 to this mechanism is added to each conductance object in the neuron (Figure 3I). Setting all maximal
243 conductance densities to some low value and integrating the model shows that the intracellular Calcium
244 levels rise over time and approach the target Calcium concentration (Figure 3J), while all conductance
245 densities increase and then remain bounded (Figure 3K). Examining the voltage dynamics of the cell
246 reveal that it transitions from quiescence to truncated bursts of action potentials to periodic bursting as
247 this mechanism regulates the neuron’s ion channel spectrum. In summary, xolotl can be used to construct
248 neuron models with intracellular mechanisms such as Calcium influx and buffering, and homeostatic
249 regulation.

3.4 USING SNAPSHOTS TO EXPLORE MODEL DYNAMICS AND PARAMETERS

250 Switching back and forth points in parameter space and state space of a neuron model is a common occur-
251 rence in working with neuron models, and a significant fraction of a modeler’s time is spent in a feedback
252 loop of running simulations, viewing the output, changing parameters, and re-running simulations (De
253 Schutter 1992). Xolotl makes it easy to bookmark configurations of a model and return to them at will.
254 Internally, xolotl uses the `serialize` method to gather all parameters and dynamic variables into a vec-
255 tor of values that is passed to the underlying C++ implementation. A paired `deserialize` method is
256 used to update all parameters and variables in the object tree from this vector. This architecture provides
257 a natural framework for representing the state of any model, no matter how complex, using a vector of
258 numbers. The `snapshot` method built into xolotl leverages this schema to save the entire state of the
259 model in a named variable, that can be accessed using another built-in method called `reset`.

260 (Figure 4) illustrates how these features can be used to explore the dynamics of the model presented
261 in the previous section. First, the current state of the model is saved using the `snapshot` method into
262 a state called “initial”. In this state, the model exhibits periodic bursting activity due to a particular con-
263 figuration of maximal conductance densities (Figure 3, orange). On setting the maximal conductances of
264 the Calcium-permissive channels to 0, the model switches to a tonic spiking activity (Figure 3, purple).
265 Integrating the model for a longer duration allows the homeostatic control mechanism in the cell to restore
266 the conductance profile and bursting activity to a state close to the original state (Figure 3, green). This
267 state is saved using the name “final”.

268 The initial state can be returned to using the `reset` method, and a new manipulation to the model can
269 be explored. Here, the intracellular Calcium target is modified, and the model is re-integrated, to yield
270 a different voltage activity (Figure 3, blue). At the end of this numerical exploration, any of the saved
271 states can be quickly returned to using the `reset` method, making the process of re-initializing models
272 to desired states and parameters both error-free and efficient.

3.5 SIMULATING NETWORK MODELS

273 Neurons communicate and interact using synapses, electrochemical junctions between cells (Gjorgjieva,
274 Drion, and Marder 2016; Hua and Smith 2004). In chemical synapses, the presynaptic neuron releases

275 packets of neurotransmitter across the synaptic cleft, which activate receptors on the postsynaptic neuron.
276 In electrical synapses, no chemical intermediary is involved. New patterns of activity can emerge from
277 the characteristics of the connecting synapses (Li, Bucher, and Nadim 2018; Nadim et al. 1999; Gutierrez
278 and Marder 2013; Gutierrez, O’Leary, and Marder 2013).

279 Network models in xolotl consist of compartment objects that can be connected by synapse objects.
280 Two compartments representing different neurons can be connected using synapses using the built-in
281 `connect` method. For example, to connect two single-compartment neurons called `LP` and `PY` using a
282 chemical synapse of type `Cholinergic` with strength 30 nS, we can use

```
283 x.connect('LP', 'PY', 'Cholinergic', 'gbar', 30);
```

284 Xolotl has several types of synapses built-in, and other synapse classes can be easily added using
285 templates. Figure 5 demonstrates the implementation of a model of the triphasic pyloric rhythm in the
286 stomatogastric ganglion of crustaceans (Prinz, Bucher, and Marder 2004). The pyloric model contains
287 three compartments (`AB`, `LP`, and `PY`) and seven synapses (Figure 5A). This structure is recapitulated in
288 the hierarchy of the xolotl object, where conductances are contained within compartments (Figure 5B).
289 The membrane potentials show triphasic rhythmicity in the three compartments (Figure 5C-E). When the
290 `PY` is depolarized, the dynamical variable mediating the glutamatergic (`Glut`) synapse model between
291 `PY` and `LP` is close to 1 and `LP` is inhibited (Figure 5F). Conversely, when `PY` is hyperpolarized, the
292 dynamical variable is close to 0. In this model, when `PY` spikes, IPSPs can be seen in the `LP` voltage trace
293 (Figure 5D-E).

3.6 USING THE GUI TO MANIPULATE PARAMETERS

294 Conductance-based neuron models are typically high dimensional and contain many parameters. Chang-
295 ing a single parameter monotonically can cause non-monotonic changes in behavior of the model, and
296 certain dynamical features may only emerge when in specific non-convex regions of parameter space
297 (Golowasch et al. 2002). It is often challenging to build intuition about what effect a parameter has on the
298 model under these conditions. Traditionally, the technique used by computational neuroscientists in build-
299 ing intuition about these models is to iteratively run simulations, view outputs and change parameters. In
300 practice, this meant writing a script, running it, inspecting the output, changing parameters in the script,
301 and repeating this process. It can be cumbersome, and every step in this process involves “mode” changes:
302 switching between a text editor, viewing a graphical output, and the command line that can frustrate the
303 researcher.

304 Xolotl is designed to streamline this process and allows for any parameter in any model to be ma-
305 nipulated using graphical sliders, with immediate, real-time feedback of its behavior. Any model in the
306 simulator can be manipulated using

```
307 x.manipulate
```

308 This method creates a GUI element with sliders for every parameter, and also creates a set of plots that
309 shows the dynamical behavior of the model (Fig. 6). By default, time series of the voltage and the calcium
310 of every compartment are shown, though this can be modified. Moving any of the sliders updates the value
311 of that parameter in the model, and also triggers a function call that reintegrates the model and updates the
312 output plots. This function call can also update custom plots, like the one shown in (Fig. 6B). Any model
313 can be manipulated in this way without writing any additional code.

314 This feature was only possible due to our architectural decision to split the code base across two pro-
315 gramming environments. A rich scientific programming environment like MATLAB makes it possible to
316 easily generate user interface elements and to bind them to data in plots, while the sheer speed of compiled
317 languages like C++ allow for the immediate, real-time feedback and updating of plots. By default, any
318 parameter in the model can be manipulated, including parameters in user-defined mechanisms that do not

319 exist in the base simulator. The GUI can be constrained to arbitrary subsets of model parameters using
320 wild card matching (as shown in Fig. 6) or by manually specifying the parameters of interest.

4 BENCHMARKS

321 Our goal in designing xolotl was to create an easy-to-use neuron and network simulator that was fast
322 enough and accurate enough for routine use by computational neuroscientists. In this section, we bench-
323 marked the speed and accuracy of xolotl in simulating single and large numbers of Hodgkin-Huxley-like
324 neuron models (as in Fig. 1) and bursting neuron models based on the bursting neurons in the lobster
325 stomatogastric ganglion (STG) (Prinz, Bucher, and Marder 2004). For each type of neuron model, we
326 compared our software to NEURON (Hines and Carnevale 1997), a high-performance and powerful neu-
327 ron simulator specialized in simulating neurons with complex morphologies and DynaSim (Sherfey et
328 al. 2018), a general-purpose simulator that can solve coupled differential equations numerically. All
329 simulators were run on the same hardware using fixed time-step solvers: xolotl used the Exponential
330 Euler method (Dayan and Abbott 2001), NEURON used the implicit Euler solver (Hines and Carnevale
331 1997) and DynaSim used C-compiled 2nd-order Runge-Kutta integration scheme as recommended for
332 high-performance (Sherfey et al. 2018). We measured the speed of each simulator by dividing the time
333 simulated for, by the time it took for the simulator to complete integration. For example, if a simulator
334 could simulate 10 seconds of model data in 1 second, its speed would be 10X. We measured the speed of
335 every simulator as a function of simulation time step, total length of simulation, and system size.

336 All three simulators were faster with larger time steps, since fewer iterations were needed (Fig. 7A-B),
337 and were approximately linear in the region tested. Xolotl compared favorably to NEURON and DynaSim
338 in this task. We also measured the quality of the simulated output by comparing it to the simulated output
339 at the smallest time step. Simulation error was measured using the LeMasson cost (LeMasson and Maex
340 2000), and was comparable amongst the three simulators (Fig. 7C-D). Since xolotl sets up and runs the
341 simulation in C++, it needs to transfer parameters and data to and from the underlying implementation.
342 To measure the performance cost of this overhead, we repeated these benchmarks on all three simulators
343 at a fixed time step of 0.1 ms and varied the length of time simulated for. Speed increased with simulation
344 duration up to a point, and then saturated, indicating a fixed performance cost to the overhead (Figure
345 7E-F, black lines). Simulations using DynaSim, which also used a similar architecture and need to move
346 data between C implementations and the MATLAB workspace, showed a similar increase in speed with
347 simulation length (Figure 7E-F, red lines). However, simulations using NEURON ran at a constant speed
348 irrespective of simulation length, presumably due to differences in the underlying implementation (Figure
349 7E-F, blue lines).

350 Many simulators have been designed with a focus on simulate large numbers of compartments, either
351 as networks with many identical neurons or in a large multi-compartment neuron model (Brette et al.
352 2007; Sherfey et al. 2018; Vitay, Dinkelbach, and Hamker 2015; Delorme and Thorpe 2003). While our
353 software is not designed for this task *per se*, we measured its performance as a function of the number of
354 compartments simulated. Xolotl can quickly create a number of identical copies of a compartment using
355 the `replicate` method:

```
356 x.replicate('compartment_to_replicate', n_copies);
```

357 We used the `replicate` method to create and run models with varying numbers of neurons (either
358 Hodgkin-Huxley-like or bursting neurons) and measured the speed of all three simulators as a function of
359 system size. Plotting the speed normalized by the system size vs. the system size, we observed that the
360 speed of integration of xolotl is linear with system size (Figure 7G-H, black lines), for up to 1000 single-
361 compartment neurons (up to 13,000 ODEs). Its performance compares favorably with that of NEURON
362 and DynaSim as a function of system size (Figure 7G-H).

5 DISCUSSION

363 We set out to design a neuron and network simulator that could be useful in the classroom setting, espe-
364 cially for students of computational neuroscience, while also being powerful, fast, and extensible enough
365 to be used for research. By using a novel architecture that permits the symbolic manipulation of C++ ob-
366 jects in a intuitive MATLAB interface, we demonstrated some of the features of xolotl using simulations
367 of single-compartment models of Hodgkin-Huxley like neurons (Fig. 1); voltage clamp experiments to
368 recover activation functions of single channel types (Fig. 2); a neuron model where intracellular mech-
369 anisms can control the dynamics of Calcium and can regulate the maximal conductance of ion channel
370 types in an activity-dependent manner (Fig. (3)); and a network of neurons with multiple synapse types
371 (Fig. 5). We also illustrated how built-in features of the simulator make it easy to bookmark and jump
372 between model configurations (Fig. 3, purple), and how parameters of the model can be changed using
373 sliders and their effect can be viewed in real time (Fig. 6).

5.1 A FOCUS ON USABILITY

374 “About half the time spent on a typical simulation project involves creating and tuning the model. Thus,
375 a good user interface may contribute more to the overall efficiency of a project than pure computation
376 speed.” (De Schutter 1992). Xolotl is designed primarily with ease-of-use in mind. This includes the time
377 it takes to install, setup, and learn how to use the software, the time to write and debug scripts, and the time
378 to perform the simulations (Rudolph and Destexhe 2007). An easy-to-use simulation environment must
379 minimize time spent in all these domains, especially during human engagement with the software. Com-
380 plicated software remains broadly inaccessible and time-consuming even to perform single-compartment
381 simulations, though the actual simulation time may be very small.

382 We have focussed on making our software as easy to use as possible, without sacrificing performance or
383 extensibility. For example, the software and all dependencies can be installed using a single-line installer
384 script from within the MATLAB command line. The installation includes worked example scripts that
385 demonstrate various features of the simulator, that can be run without any configuration. We decided
386 to built the the front-end interface to xolotl in MATLAB to facilitate interoperability with existing tools
387 for time series analysis, optimization, and parallel computing. This allowed us to build rich tools for
388 visualization and to interact with the simulation.

5.2 COMPARISON WITH OTHER SIMULATORS

389 Over the years, several simulators have been developed to integrate systems of coupled differential equa-
390 tions that model the spiking activity of neurons (Brette et al. 2007; Sherfey et al. 2018; Vitay, Dinkelbach,
391 and Hamker 2015; Delorme and Thorpe 2003; Hines and Carnevale 1997; Bower, Beeman, and Hucks
392 2003). A critical architectural choice in designing a simulator is how much “scaffolding” a user is pro-
393 vided with to construct a model; whether a model is specified by equations or by components, or by some
394 combination of the two. In an equation-oriented architecture, the user starts with a blank slate and the
395 primary method of specifying a model is to write out its differential equations (Stimberg et al. 2014b). In
396 contrast, in a component-oriented architecture, the primary method of specifying a model is to assemble
397 it from pre-existing components, each of which include differential equations, parameters, and solvers.
398 Both approaches have advantages and disadvantages that are discussed below.

399 An equation-oriented simulator can be more transparent and allows the user to know exactly what is
400 being solved, but equations can be cumbersome to write out, read, or to debug. In most commonly used
401 programming environments, these equations have to be entered as strings, and complex parsing has to be
402 carried out by the simulator to check that these strings constitute valid equations. In addition, parameters
403 have to be written explicitly into equations, and it is usually not trivial to change parameters after initial
404 specification. In contrast, components are easy to assemble into a model, but it can be hard to know what
405 they contain, where they are physically located on the user’s computer, and how they can be changed.

406 NEURON is primarily a component-oriented neuronal simulator, and new components are specified in
407 special model files that can be “inserted” into a model. BRIAN is an equation-oriented neuronal simulator
408 meant to be used from within Python (Goodman and Brette 2009). XPP is a general purpose dynamical
409 system simulator that is equation-oriented (Ermentrout 2002). DynaSim is an equation-oriented simulator
410 with some component-oriented capabilities. Models can be specified by both strings of equations or com-
411 ponents, but since models do not exist as objects in the workspace, parameters and variables have to be
412 reinitialized when changed (Sherfey et al. 2018).

413 Xolotl is a purely component-based simulator, and all equations need to be included in a C++ header file
414 that specifies a object. Since our automatic type system binds MATLAB objects to the underlying C++
415 header files, objects can be inspected and parameters can be modified in the MATLAB workspace. To
416 mitigate some of the drawbacks of the component-oriented paradigm, we have implemented an architec-
417 ture that allows the user to access the underlying C++ code of any object by simply clicking on the object
418 tree in the MATLAB command line. This feature removes the uncertainty inherent in other component-
419 oriented simulators of the equations underlying each component, and allows the user to modify these
420 equations if needed.

421 Another architectural choice in designing simulators is the syntax required for specifying models.
422 Equation-oriented simulators specify models as strings of equations, so must invent a new syntax to
423 specify derivatives, variables, and other common elements in coupled differential equations. Some
424 component-oriented simulators like NEURON also specify their own syntax, or have invented their own
425 language to specify components and write out equations. While this allows for powerful features such
426 as support for units in NEURON, the user is required to learn a novel syntax and vocabulary, hindering
427 ease of use. In general, the syntax for model specification in different simulators can be different. For
428 example, DynaSim, BRIAN, XPP, and NEURON all use different, incompatible formalisms to represent
429 equations, increasing the cognitive load on users using more than one simulator. Here, we have elected not
430 to specify a domain-specific “middleware” layer, and instead specify and implement models and equations
431 in idiomatic C++. This greatly decreases the learning curve and allows users with a general familiarity
432 with programming languages to quickly acquaint themselves even with the most technical parts of the
433 simulator.

5.3 AUDITABILITY AND REPRODUCIBILITY

434 The use of computational tools is increasingly central to the scientific method; yet, the lack of auditability
435 and accountability in their use has led to a crisis of credibility affecting many scientific fields (Stodden
436 et al. 2016; Baker 2016). Unlike in experimental research, where a lack of reproducibility can manifest
437 due to meaningful reasons like uncharted differences in experimental protocols or intrinsic variability,
438 the reasons for irreproducibility in computational research are often trivial and include: a) typographical
439 errors from transcribing model parameters and equations, b) obscure software design that leads to users not
440 knowing precisely what equations the software is solving, or what parameters it is using, c) incompatibility
441 with version control systems and rolling software development that leads to ambiguity in which the version
442 of the software that was used to generate a particular result is unclear, and d) convoluted architectures that
443 make it too complex for non-experts to understand the inner workings of the software (Xu, Xu, and Deng
444 2017; Sedano 2016; Vikström 2009).

445 Our software was designed with this threat model in mind, and has features that allow the user to answer
446 the following questions in the affirmative: “Can I be sure that I am doing what I think I am doing?” and “Is
447 it possible for others to reproduce *exactly* what I have just done?”. Our goal was to design software that
448 would allow the user to verify for herself that the software was running as she intended, and to be able to
449 reproduce results from others quickly and unambiguously. The primary design choice in our software that
450 enables auditability and reproducibility is that every simulation is tied to an alphanumeric checksum, or
451 hash, using the MD5 algorithm (Rivest 1992). The hash is computed from every C++ file that is part of the
452 model, and any changes in any C++ file included in the model will trigger a recompilation of that model.
453 Thus, the hash guarantees that a given model is derived from a set of source files, obviating any ambiguity

454 about the code used to generate a model. In addition, every parameter and state variable in the model
455 can also be hashed together with underlying code, allowing the user to generate a short checksum that
456 guarantees with high probability that every aspect of the model – code, parameters, and initial conditions
457 – are exactly as they should be.

458 Typographical errors from transcribing model parameters and equations can also be detected using
459 hashes, and the component-oriented architecture of our software makes it easy to debug code and spot
460 errors. Our software has been designed so that it is possible to explore the model interactively in the com-
461 mand line, and it is possible to “click through” from the highest level of the model in the command line all
462 the way down to the underlying code of any component in the model. This design allows the user to know
463 precisely the equations being solved, and view the code that numerically integrates them. Finally, the core
464 of our software is written in a few hundred lines of code and contains just four classes: compartments,
465 conductances, synapses, and mechanisms. This architectural simplicity lets a motivated user understand
466 the entirety of our code quickly.

5.4 OUTLOOK AND FUTURE DIRECTIONS

467 In its current form, xolotl is an efficient and easy to use neuron and network simulator that is actively be-
468 ing used in research. Results from an early version of this simulator guided intuition in the modeling of a
469 recently characterized Calcium-dependent Potassium channel found in *Drosophila* neuromuscular presy-
470 naptic terminals (Bronk et al. 2018). Work on the simulator continues in the open at a publicly accessible
471 repository (<https://github.com/sg-s/xolotl/>), and the library of conductances, synapses and mechanisms
472 that xolotl ships with grows continuously. While this simulator was intended as a research tool, the many
473 worked examples that are built into it demonstrate how it could also be used as a teaching tool.

474 Because xolotl models are bonafide MATLAB objects, they are compatible with most of the powerful
475 tools that exist within MATLAB. For example, it is possible to write simple scripts that run xolotl models
476 in parallel using MATLAB’s parallel processing toolbox, speeding up large simulations. Xolotl models are
477 also compatible with the global optimization toolbox in MATLAB, allowing parameters in xolotl models
478 to be optimized, enabling the creation of toolboxes that efficiently tune parameters in neuron models to
479 satisfy arbitrary constraints (Achard and De Schutter 2006; Krichmar 2014; Keren, Peled, and Korngreen
480 2005; Van Geit 2007; Druckmann et al. 2008).

481 Care has been taken to reduce the amount of technical debt (Suryanarayana, Samarthiyam, and Sharma
482 2014) associated with this project, with all parts of the simulator and dependencies written in a modular,
483 objected oriented fashion. As a result, many of the key features and architectures of xolotl can be reused
484 by others in their own applications. For example, cpplab, the automatic type system that binds C++
485 code to MATLAB objects, is independent of this simulator, and exists as a distinct repository that has
486 been made freely available (<https://github.com/sg-s/cpplab/>); and the framework for generating a GUI with
487 sliders for each parameter that is hooked up to function callbacks also exists as an independent repository
488 (<https://github.com/sg-s/puppeteer/>) that can be easily integrated into other applications.

CONFLICT OF INTEREST STATEMENT

489 The authors declare that the research was conducted in the absence of any commercial or financial
490 relationships that could be construed as a potential conflict of interest.

AUTHOR CONTRIBUTIONS

491 SG-S & AH wrote the software and created the online user documentation. EM provided general
492 oversight. All authors wrote and reviewed the paper.

FUNDING

493 The authors acknowledge funding from the National Institutes through R90DA033463 (AH),
494 T32NS007292-31 (SG-S) and R35 NS097343 (EM).

ACKNOWLEDGMENTS

495 The authors would like to thank Timothy O’Leary and Leandro Alonso for useful discussions, Janis Li
496 for help transcribing many conductance models, and members of the Marder Lab, especially Sonal Kedia,
497 Ekaterina Morozova, Jason Pipkin and Philipp Rosenbaum for careful reading of the manuscript.

DATA AVAILABILITY STATEMENT

498 The code to generate all figures is available at ([https://github.com/marderlab/](https://github.com/marderlab/xolotl-paper)
499 [xolotl-paper](https://github.com/marderlab/xolotl-paper)). xolotl is freely available at (<https://github.com/sg-s/xolotl>).

REFERENCES

- 500 Achard, Pablo and Erik De Schutter (2006) “Complex Parameter Landscape for a Complex Neuron
501 Model”. English. In: *PLoS Computational Biology* 2.7, e94–11. DOI: 10.1371/journal.pcbi.
502 0020094.
- 503 Baker, Monya (2016) “Why Scientists Must Share Their Research Code”. In: *Nature*. DOI: 10.1038/
504 nature.2016.20504.
- 505 Bower, James M David Beeman, and Michael Hucks (2003) “The genesis simulation system”. In:
506 Brette, Romain, Michelle Rudolph, Ted Carnevale, Michael Hines, David Beeman, James M. Bower, et al.
507 (2007) “Simulation of Networks of Spiking Neurons: A Review of Tools and Strategies”. In: *Journal of*
508 *Computational Neuroscience* 23.3, pp. 349–398. DOI: 10.1007/s10827-007-0038-6.
- 509 Bronk, Peter, Elena A Kuklin, Srinivas Gorur-Shandilya, Chang Liu, Timothy D Wiggin, Martha L Reed,
510 et al. (2018) “Regulation of Eag by Ca²⁺/calmodulin controls presynaptic excitability in *Drosophila*”.
511 In: *Journal of neurophysiology* 119.5, pp. 1665–1680.
- 512 Cole, Kenneth (1955) “Ions, Potentials, and the Nerve Impulse”. In: *Electrochemistry in Biology and*
513 *Medicine*. Ed. by Theodore Shedlovsky. New York: Wiley, pp. 121–140.
- 514 Cole, Kenneth S. and John W. Moore (1960) “Ionic Current Measurements in the Squid Giant Axon
515 Membrane”. In: *The Journal of General Physiology* 44.1, pp. 123–167.
- 516 Davison, Andrew P., Daniel Brüderle, Jochen M. Eppler, Jens Kremkow, Eilif Muller, Dejan Pecevski,
517 et al. (2009) “PyNN: A Common Interface for Neuronal Network Simulators”. In: *Frontiers in*
518 *Neuroinformatics* 2. DOI: 10.3389/neuro.11.011.2008.
- 519 Dayan, Peter and L. F. Abbott (2001) *Theoretical Neuroscience*. Computational neuroscience. Cambridge,
520 Mass.: Massachusetts Institute of Technology Press. xv+460.
- 521 De Schutter, Erik (1992) “A Consumer Guide to Neuronal Modeling Software”. In: *Trends in Neuro-*
522 *sciences* 15.11, pp. 462–464. DOI: 10.1016/0166-2236(92)90011-V.
- 523 Delorme, Arnaud and Simon J. Thorpe (2003) “SpikeNET: An Event-Driven Simulation Package for
524 Modelling Large Networks of Spiking Neurons”. In: *Network: Computation in Neural Systems* 14.4,
525 pp. 613–627. DOI: 10.1088/0954-898X_14_4_301.
- 526 Druckmann, Shaul, Thomas K Berger, Sean Hill, Felix Schürmann, Henry Markram, and Idan Segev
527 (2008) “Evaluating automated parameter constraining procedures of neuron models by experimental and
528 surrogate data”. English. In: *Biological cybernetics* 99.4-5, pp. 371–379. DOI: 10.1007/s00422-
529 008-0269-2.
- 530 Ermentrout, Bard (2002) *Simulating, analyzing, and animating dynamical systems: a guide to XPPAUT*
531 *for researchers and students*. Vol. 14. Siam.

- 532 Gjorgjieva, Julijana, Guillaume Drion, and Eve Marder (2016) “Computational Implications of Biophys-
533 ical Diversity and Multiple Timescales in Neurons and Synapses for Circuit Performance”. In: *Current*
534 *Opinion in Neurobiology* 37, pp. 44–52. DOI: 10.1016/j.conb.2015.12.008.
- 535 Golowasch, Jorge, Mark S Goldman, LF Abbott, and Eve Marder (2002) “Failure of averaging in the
536 construction of a conductance-based neuron model”. In: *Journal of Neurophysiology* 87.2, pp. 1129–
537 1131.
- 538 Goodman, Dan F. M. and Romain Brette (2009) “The Brian Simulator”. In: *Frontiers in Neuroscience* 3.
539 DOI: 10.3389/neuro.01.026.2009.
- 540 Gratiy, Sergey L Yazan N Billeh, Kael Dai, Catalin Mitelut, David Feng, Nathan W Gouwens, et al.
541 (2018) “BioNet: A Python interface to NEURON for modeling large-scale networks”. In: *PloS one*
542 13.8, e0201630.
- 543 Gutierrez, Gabrielle J. and Eve Marder (2013) “Rectifying Electrical Synapses Can Affect the Influence
544 of Synaptic Modulation on Output Pattern Robustness”. In: *Journal of Neuroscience* 33.32, pp. 13238–
545 13248. DOI: 10.1523/JNEUROSCI.0937-13.2013.
- 546 Gutierrez, Gabrielle J., Timothy O’Leary, and Eve Marder (2013) “Multiple Mechanisms Switch an Elec-
547 trically Coupled, Synaptically Inhibited Neuron between Competing Rhythmic Oscillators”. In: *Neuron*
548 77.5, pp. 845–858. DOI: 10.1016/j.neuron.2013.01.016.
- 549 Hines, M. L. and N. T. Carnevale (1997) “The NEURON Simulation Environment”. In: *Neural*
550 *Computation* 9.6, pp. 1179–1209. DOI: 10.1162/neco.1997.9.6.1179.
- 551 Hines, Michael (1984) “Efficient Computation of Branched Nerve Equations”. In: *International Journal*
552 *of Bio-Medical Computing* 15.1, pp. 69–76. DOI: 10.1016/0020-7101(84)90008-4.
- 553 Hines, Michael, Andrew P. Davison, and Eilif Muller (2009) “NEURON and Python”. In: *Frontiers in*
554 *Neuroinformatics* 3. DOI: 10.3389/neuro.11.001.2009.
- 555 Hodgkin, A. L. and A. F. Huxley (1952a) “A Quantitative Description of Membrane Current and Its
556 Application to Conduction and Excitation in Nerve”. In: *The Journal of Physiology* 117.4, pp. 500–544.
- 557 — (1952b) “The Components of Membrane Conductance in the Giant Axon of Loligo”. In: *The Journal*
558 *of Physiology* 116.4, pp. 473–496.
- 559 Hodgkin, A. L., A. F. Huxley, and B. Katz (1952) “Measurement of Current-Voltage Relations in the
560 Membrane of the Giant Axon of Loligo”. In: *The Journal of Physiology* 116.4, pp. 424–448.
- 561 Hodgkin, A. L. and B. Katz (1949) “The Effect of Sodium Ions on the Electrical Activity of the Giant
562 Axon of the Squid”. In: *The Journal of Physiology* 108.1, pp. 37–77.
- 563 Hua, Jackie Yuanyuan and Stephen J. Smith (2004) “Neural Activity and the Dynamics of Central Nervous
564 System Development”. In: *Nature Neuroscience* 7.4, pp. 327–332. DOI: 10.1038/nn1218.
- 565 Hull, Michael James and David J. Willshaw (2014) “Morphforge: A Toolbox for Simulating Small Net-
566 works of Biologically Detailed Neurons in Python”. In: *Frontiers in Neuroinformatics* 7. DOI: 10.
567 3389/fninf.2013.00047.
- 568 Keren, Naomi, Noam Peled, and Alon Korngreen (2005) “Constraining Compartmental Models Using
569 Multiple Voltage Recordings and Genetic Algorithms”. English. In: *Journal of Neurophysiology* 94.6,
570 pp. 3730–3742. DOI: 10.1152/jn.00408.2005.
- 571 Kispersky, Tilman J., Jonathan S. Caplan, and Eve Marder (2012) “Increase in Sodium Conductance
572 Decreases Firing Rate and Gain in Model Neurons”. In: *Journal of Neuroscience* 32.32, pp. 10995–
573 11004. DOI: 10.1523/JNEUROSCI.2045-12.2012.
- 574 Krichmar, Jeffrey L (2014) “An efficient automated parameter tuning framework for spiking neural
575 networks”. In: pp. 1–15. DOI: 10.3389/fnins.2014.00010/abstract.
- 576 LeMasson, Gwendal and Reinoud Maex (2000) “Introduction to Equation Solving and Parameter Fitting”.
577 In: *Computational Neuroscience: Realistic Modeling for Experimentalists*. Ed. by Erik de Schutter. CRC
578 Press, p. 25.
- 579 Li, Xinpeng, Dirk M. Bucher, and Farzan Nadim (2018) “Co-Modulation of Synapses and Voltage-Gated
580 Ionic Currents by Combined Actions of Multiple Neuromodulators Follow Distinct Rules”. In: *bioRxiv*,
581 p. 265694. DOI: 10.1101/265694.
- 582 Liu, Zheng, Jorge Golowasch, Eve Marder, and L. F. Abbott (1998) “A Model Neuron with Activity-
583 Dependent Conductances Regulated by Multiple Calcium Sensors”. In: *Journal of Neuroscience* 18.7,
584 pp. 2309–2320. DOI: 10.1523/JNEUROSCI.18-07-02309.1998.

- 585 MacLean, Jason N., Ying Zhang, Bruce R. Johnson, and Ronald M. Harris-Warrick (2003) “Activity-
586 Independent Homeostasis in Rhythmically Active Neurons”. In: *Neuron* 37.1, pp. 109–120. DOI: 10 .
587 1016/S0896-6273(02)01104-2.
- 588 Marder, Eve and L. F. Abbott (1995) “Theory in Motion”. In: *Current Opinion in Neurobiology* 5.6,
589 pp. 832–840.
- 590 Nadim, Farzan, Yair Manor, Nancy Kopell, and Eve Marder (1999) “Synaptic Depression Creates a Switch
591 That Controls the Frequency of an Oscillatory Circuit”. In: *Proceedings of the National Academy of*
592 *Sciences* 96.14, pp. 8206–8211. DOI: 10.1073/pnas.96.14.8206.
- 593 O’Leary, Timothy, Alex H. Williams, Jonathan S. Caplan, and Eve Marder (2013) “Correlations in
594 Ion Channel Expression Emerge from Homeostatic Tuning Rules”. In: *Proceedings of the National*
595 *Academy of Sciences of the United States of America* 110.28, E2645–2654. DOI: 10.1073/pnas .
596 1309966110.
- 597 O’Leary, Timothy, Alex H. Williams, Alessio Franci, and Eve Marder (2014) “Cell Types, Network
598 Homeostasis, and Pathological Compensation from a Biologically Plausible Ion Channel Expression
599 Model”. In: *Neuron* 82.4, pp. 809–821. DOI: 10.1016/j.neuron.2014.04.002.
- 600 Oh, Jiyeon and Donald A. French (2006) “Error Analysis of a Specialized Numerical Method for Math-
601 ematical Models from Neuroscience”. In: *Applied Mathematics and Computation* 172.1, pp. 491–507.
602 DOI: 10.1016/j.amc.2005.02.028.
- 603 Prinz, Astrid A (2006) “Insights from Models of Rhythmic Motor Systems”. In: *Current Opinion in*
604 *Neurobiology* 16.6, pp. 615–620. DOI: 10.1016/j.conb.2006.10.001.
- 605 Prinz, Astrid A. (2010) “Computational Approaches to Neuronal Network Analysis”. In: *Philosophical*
606 *Transactions of the Royal Society B: Biological Sciences* 365.1551, pp. 2397–2405. DOI: 10.1098/
607 rstb.2010.0029.
- 608 Prinz, Astrid A., Cyrus P. Billimoria, and Eve Marder (2003) “Alternative to Hand-Tuning Conductance-
609 Based Models: Construction and Analysis of Databases of Model Neurons”. In: *Journal of Neurophysi-*
610 *ology* 90.6, pp. 3998–4015. DOI: 10.1152/jn.00641.2003.
- 611 Prinz, Astrid A., Dirk Bucher, and Eve Marder (2004) “Similar Network Activity from Disparate Circuit
612 Parameters”. In: *Nature Neuroscience* 7.12, pp. 1345–1352. DOI: 10.1038/nn1352.
- 613 Rivest, R (1992) “The MD5 Message-Digest Algorithm”. In: *RFC Editor*. DOI: 10.17487/rfc1321.
- 614 Rudolph, Michelle and Alain Destexhe (2007) “How much can we trust neural simulation strategies?” In:
615 *Neurocomputing* 70.10-12, pp. 1966–1969.
- 616 Schulz, David J., Jean-Marc Goaillard, and Eve Marder (2006) “Variable Channel Expression in Identified
617 Single and Electrically Coupled Neurons in Different Animals”. In: *Nature Neuroscience* 9.3, pp. 356–
618 362. DOI: 10.1038/nn1639.
- 619 Sedano, T. (2016) “Code Readability Testing, an Empirical Study”. In: *2016 IEEE 29th International*
620 *Conference on Software Engineering Education and Training (CSEET) 2016 IEEE 29th International*
621 *Conference on Software Engineering Education and Training (CSEET)* pp. 111–117. DOI: 10.1109/
622 CSEET.2016.36.
- 623 Sherfey, Jason S., Austin E. Soplata, Salva Ardid, Erik A. Roberts, David A. Stanley, Benjamin R.
624 Pittman-Polletta, et al. (2018) “DynaSim: A MATLAB Toolbox for Neural Modeling and Simulation”.
625 In: *Frontiers in Neuroinformatics* 12. DOI: 10.3389/fninf.2018.00010.
- 626 Sterratt, David, ed. (2011) *Principles of Computational Modelling in Neuroscience*. OCLC:
627 ocn690090171. Cambridge ; New York: Cambridge University Press. 390 pp.
- 628 Stimberg, Marcel, Dan F. M. Goodman, Victor Benichoux, and Romain Brette (2014a) “Equation-
629 Oriented Specification of Neural Models for Simulations”. In: *Frontiers in Neuroinformatics* 8. DOI:
630 10.3389/fninf.2014.00006.
- 631 Stimberg, Marcel, Dan FM Goodman, Victor Benichoux, and Romain Brette (2013) “Brian 2 - the Second
632 Coming: Spiking Neural Network Simulation in Python with Code Generation”. In: *BMC Neuroscience*
633 14 (Suppl 1) P38. DOI: 10.1186/1471-2202-14-S1-P38.
- 634 — (2014b) “Equation-oriented specification of neural models for simulations”. In: *Frontiers in neuroin-*
635 *formatics* 8, p. 6.

- 636 Stodden, Victoria, Marcia McNutt, David H. Bailey, Ewa Deelman, Yolanda Gil, Brooks Hanson, et al.
637 (2016) “Enhancing Reproducibility for Computational Methods”. In: *Science* 354.6317, pp. 1240–1241.
638 DOI: 10.1126/science.aah6168.
- 639 Suryanarayana, Girish, Ganesh Samarthyam, and Tushar Sharma (2014) *Refactoring for software design*
640 *smells: managing technical debt*. Morgan Kaufmann.
- 641 Trappenberg, Thomas P. (2010) *Fundamentals of Computational Neuroscience*. 2nd ed. OCLC:
642 ocn444383805. Oxford ; New York: Oxford University Press. 390 pp.
- 643 Turrigiano, G., G. LeMasson, and E. Marder (1995) “Selective Regulation of Current Densities Under-
644 lies Spontaneous Changes in the Activity of Cultured Neurons”. In: *The Journal of Neuroscience: The*
645 *Official Journal of the Society for Neuroscience* 15 (5 Pt 1) pp. 3640–3652.
- 646 Van Geit, Werner (2007) “Neurofitter: A parameter tuning package for a wide range of electrophysiologi-
647 cal neuron models”. In: *Frontiers in Neuroinformatics* 1, pp. 1–18. DOI: 10.3389/neuro.11.001.
648 2007.
- 649 Vikström, Alexander (2009) “A Study of Automatic Translation of MATLAB Code to C Code Using
650 Software from the MathWorks”. Lulea University of Technology. 52 pp.
- 651 Vitay, Julien, Helge Ülo Dinkelbach, and Fred H. Hamker (2015) “ANNarchy: A Code Generation Ap-
652 proach to Neural Simulations on Parallel Hardware”. In: *Frontiers in Neuroinformatics* 9. DOI: 10.
653 3389/fninf.2015.00019.
- 654 Xu, W., D. Xu, and L. Deng (2017) “Measurement of Source Code Readability Using Word Concrete-
655 ness and Memory Retention of Variable Names”. In: *2017 IEEE 41st Annual Computer Software and*
656 *Applications Conference (COMPSAC) 2017 IEEE 41st Annual Computer Software and Applications*
657 *Conference (COMPSAC) vol. 1*, pp. 33–38. DOI: 10.1109/COMPSAC.2017.166.

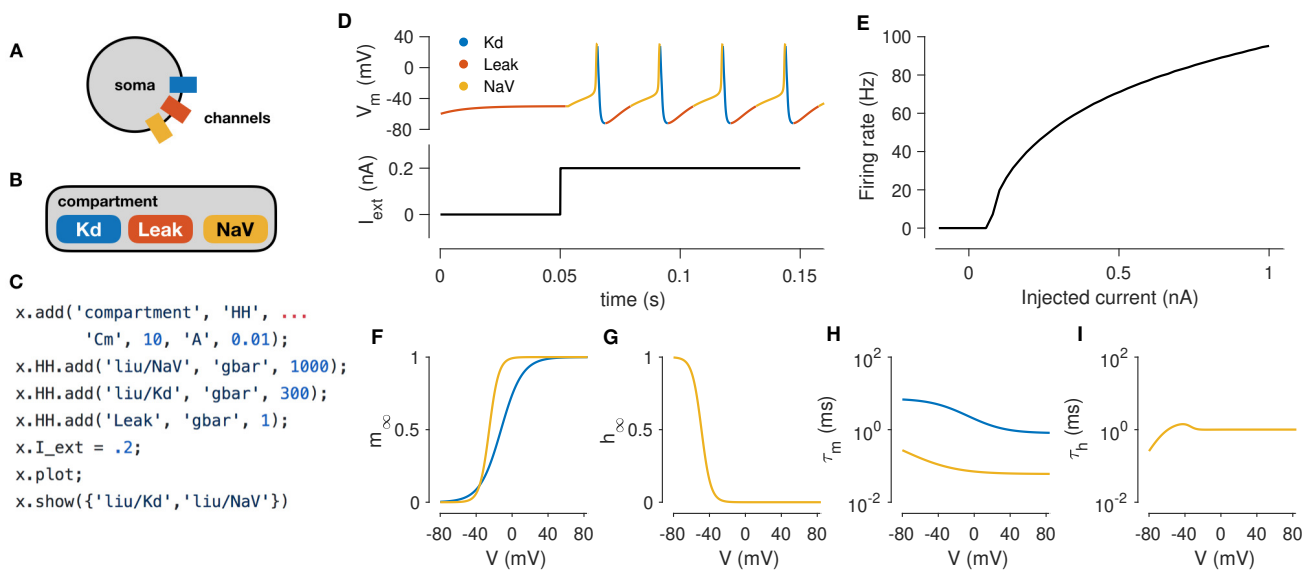


Figure 1: Simulating a single-compartment Hodgkin-Huxley spiking neuron model. (A) Schematic representation of a single-compartment neuron with three populations of ion channels (colored rectangles). (B) In xolotl, the soma is represented using an object of class “compartment” and populations of ion channels are represented by “conductance” objects contained within the compartment object. (C) The code snippet shown sets up this neuron model, injects current, integrates and plots the voltage, and displays activation functions, all in a few lines of code. (D) Simulated voltage trace of a Hodgkin-Huxley model with three conductances and 0.2 nA of injected current. Colors indicate the dominant current (gold is fast sodium (NaV), blue is delayed rectifier (Kd), red is Leak). (E) firing rate vs. current (f-I) curve of this neuron. (F-G) Steady-state gating functions for activation (m) and inactivation (h) gating variables. (H-I) Voltage-dependence of time constants for activation (m) and inactivation (h) gating variables

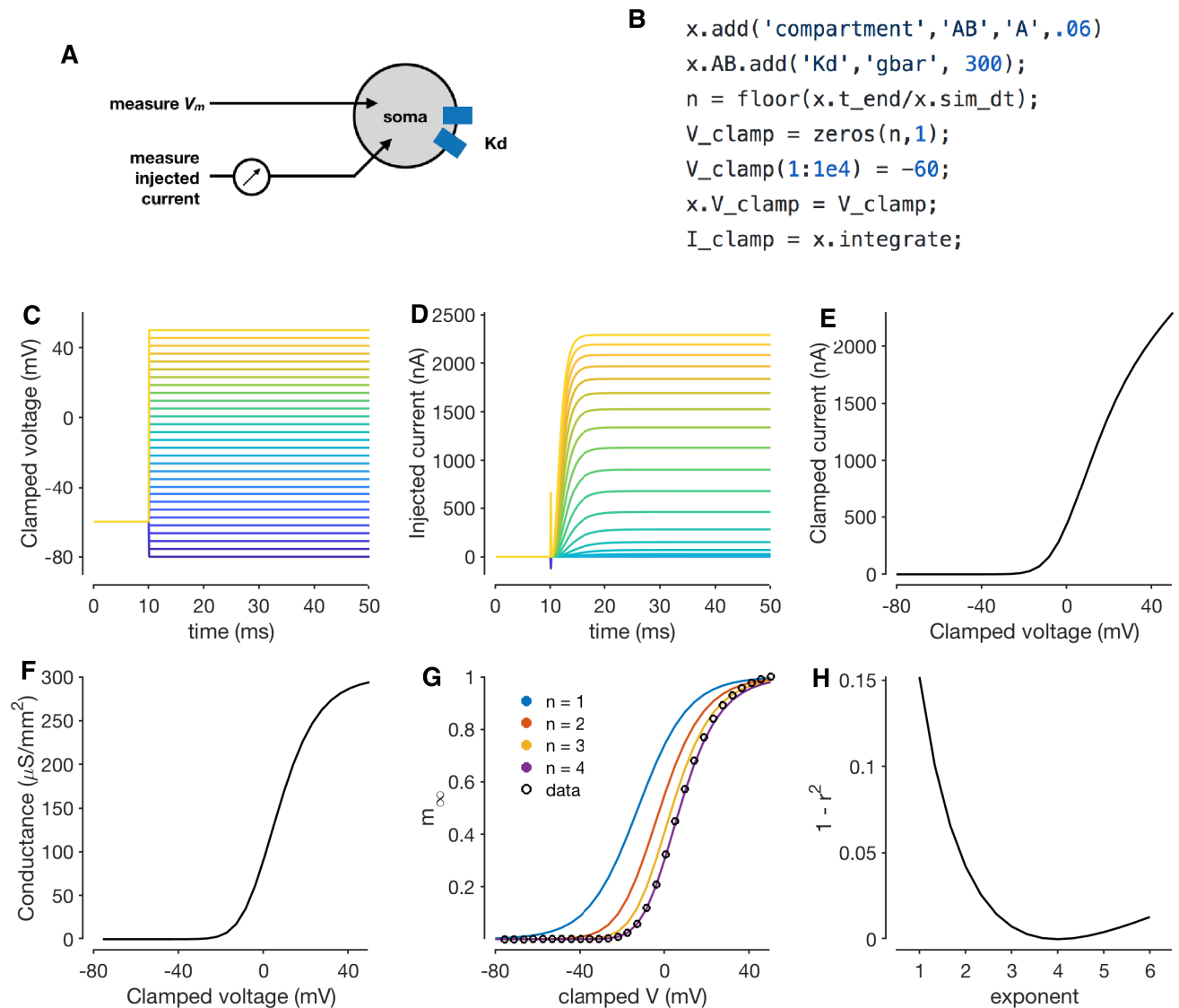


Figure 2: Simulating a voltage-clamp experiment. The diagram shows a cell with delayed rectifier potassium conductance (Liu et al. 1998) that is being recorded from in two-electrode voltage clamp (A). The code snippet shown here sets up a model with a single compartment and a single channel type, and clamps the cell to a constant voltage and integrates it (B). Voltage steps that the cell is clamped to (C). Clamp currents as a function of time (D). Asymptotic clamped current vs. clamped voltage for this cell (E). Accounting for the reversal potential of Potassium ions yields the conductance-voltage curve of this channel type (F). Normalized conductance-voltage curves, with sigmoid fits with various exponents (G). An exponent of $n = 4$ yields the best fit, allowing for the characterization of the activation function of this channel type (H).

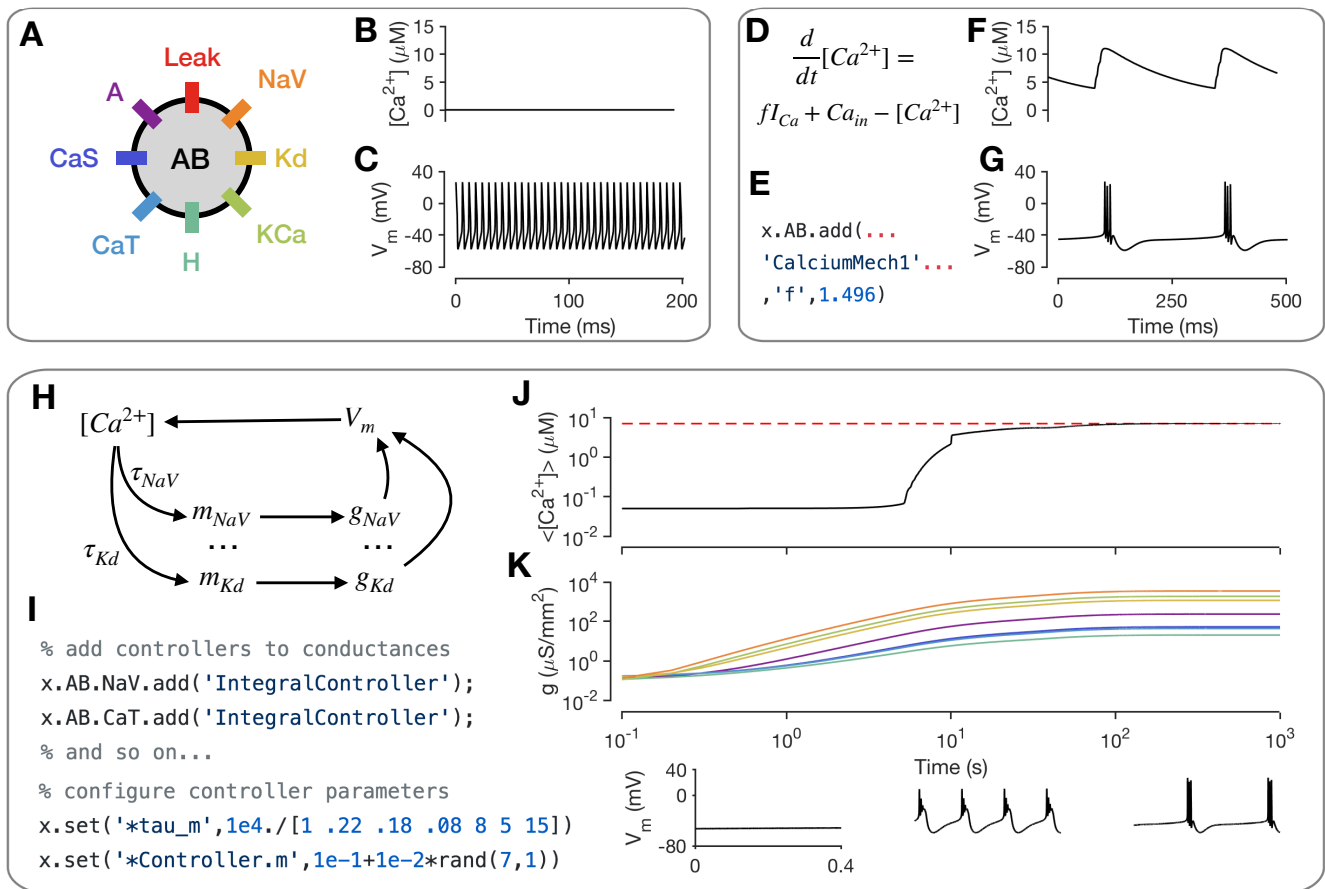


Figure 3: Modeling intracellular mechanisms. A single-compartment neuron model with 8 channel types (A). Because there is no mechanism for changing intracellular Calcium in this model, the Calcium level stays constant (B), and the cell tonically spikes (C). Intracellular Calcium buffering and influx through voltage gated Calcium channels (VGCCs) can be modeled using a simple differential equation (D). Code snippet shows how this mechanism can be added to the neuron model (E). The cell now bursts periodically, with synchronized oscillations in intracellular Calcium (F-G). Schematic of Calcium-dependent integral control homeostasis (O’Leary et al. 2013; O’Leary et al. 2014) (H). In this feedback system, the rates of mRNA synthesis depend on the Calcium level in the cell, which depends on the membrane voltage, which in turn depends on the conductance density of all channel types, which, through translation, depends on the mRNA abundance. (I) The code snippet shows how these integral controllers are implemented as mechanism objects, and can be added to conductances. (J) On integrating the model, intracellular calcium levels rise and approach the target (red dashed line). This is accompanied by an increase in the conductance densities of all channels being controlled by this homeostatic mechanism (K). The voltage behavior of the cell changes from silence to bursting with truncated spikes to regular bursting.

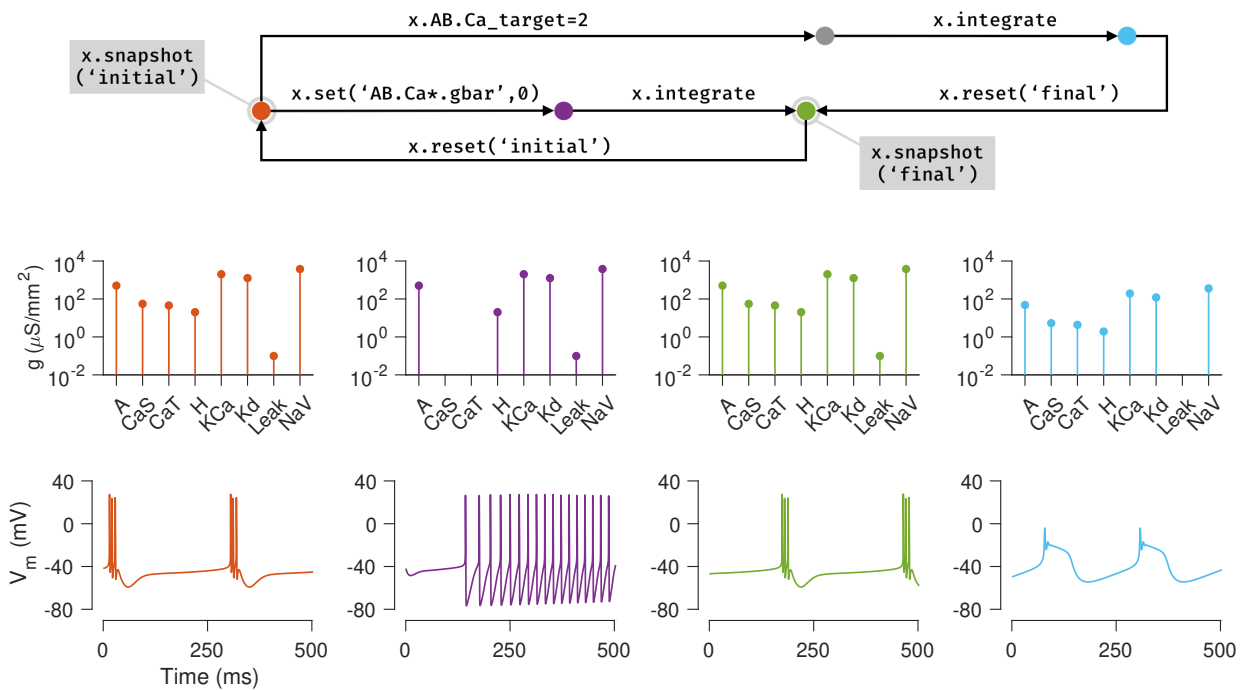


Figure 4: Snapshots allow the user to bookmark points in parameter and state space of the model and return to them *ad arbitrium*. The initial state (orange node) of the single compartment model in the previous example is saved using the `snapshot` method. This method saves all parameters and dynamic variables of the model in a named state. The first column (orange plots) shows the profile of conductances and the voltage dynamics of the model at this point at this time. The maximal conductances of the Calcium channels are then set to zero (purple node), changing the voltage dynamics of the neuron (purple plots). After evolving the model for some time (green node), the conductance profile and voltage dynamics returns to a state similar to the initial state (green plots). This configuration is now saved in a state called *final* and the initial configuration is returned to using the `reset` method (backwards arrow from green to orange). Another parameter is now changed (the Calcium target), and the model is integrated to reach a new state (blue node) where the voltage dynamics are different from the *initial* state. In summary, any state can be bookmarked using a descriptive name using the `snapshot` method, and can be returned to using the `reset` method.

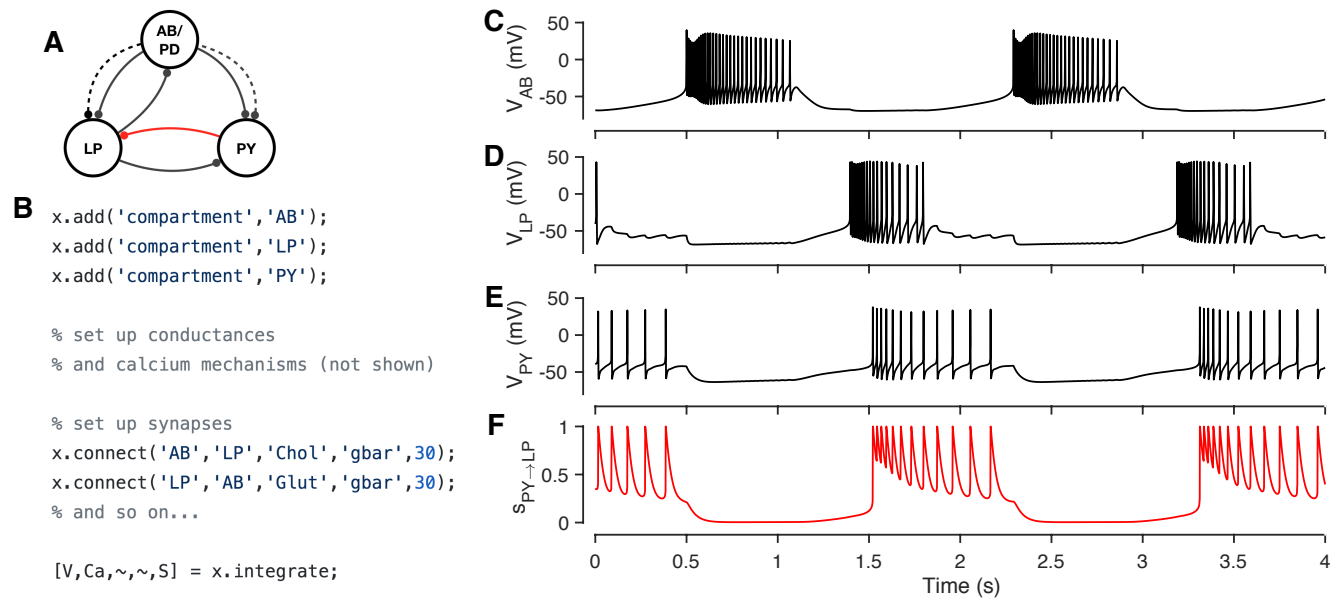


Figure 5: Simulating a network of conductance-based model neurons, coupled by voltage-dependent dynamic chemical synapses. A three-compartment model of the pyloric network in the crustacean stomatogastric ganglion (Prinz, Bucher, and Marder 2004) (A). Each neuron is modeled with a single compartment with 7-8 intrinsic conductances and 1-3 post-synaptic conductances. Synapses can be one of two types (Cholinergic (dashed lines) or Glutamatergic (solid lines)) and have different kinetics. The code snippet shows how neurons can be created, wired together using synapses, and how the model can be integrated to return voltages and intracellular calcium levels in every compartment, and the state of every synapse (B). Simulated voltage trace of a model network for the three compartments obtained from this simulation (C-E). Time series activation variable of the Glutamatergic synapse between PY and LP (red connection in diagram) shows how the synapse becomes active every time the PY neuron spikes (F).

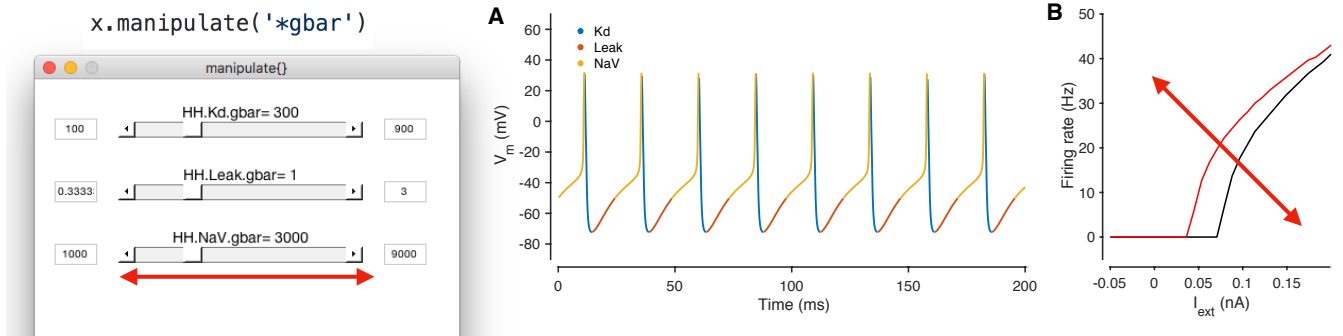


Figure 6: Manipulating neuron parameters in real time. Any set of parameter in the model can be manipulated; here, the maximal conductance of every conductance type in the model from Fig. 1 is being manipulated using the code snippet shown here. The screenshot shows a GUI with sliders for every parameter of interest that is created by the `manipulate` method. These sliders can be linked to an arbitrary number of visualization functions. In this example, two visualization functions are used: the built in `plot` method (A) and a custom function that computes the firing-rate-vs.-injected current curve for this neuron (B). Both plots refresh themselves with every movement of any slider, allowing the user to build intuition about how every parameter controls the dynamical behavior of the model. A screen recording of this model being manipulated in real time is included in Supplementary Material

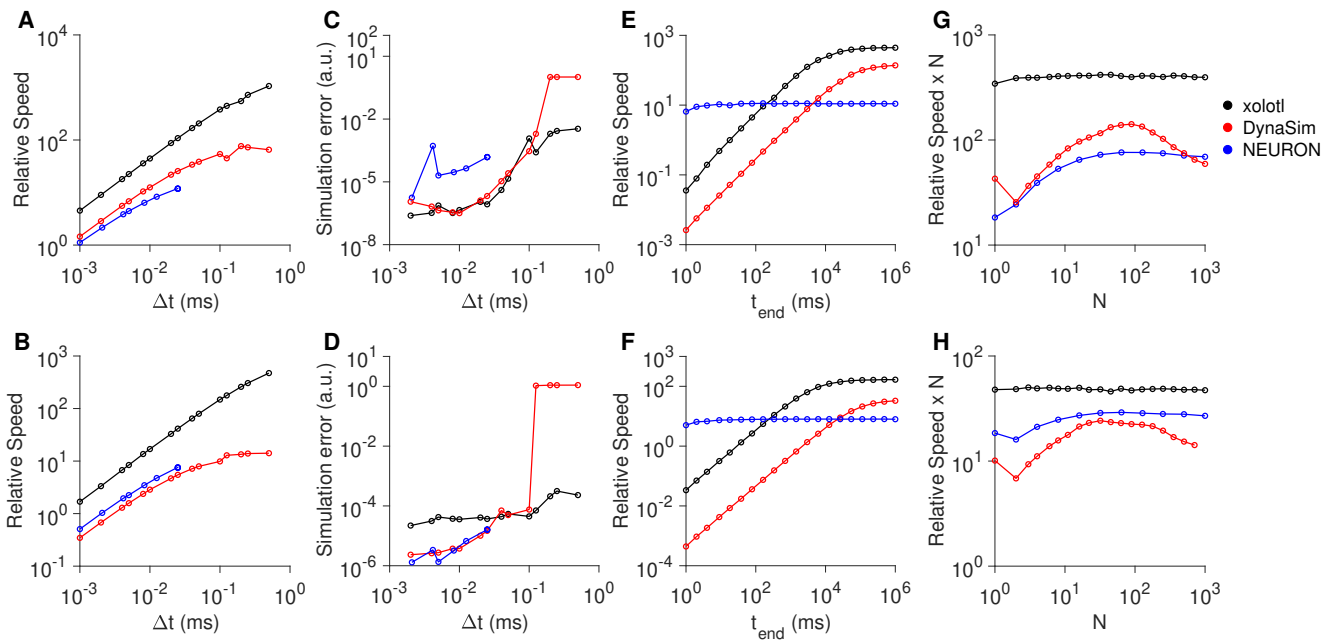


Figure 7: Comparison of speed and accuracy of xolotl, NEURON and DynaSim. The top row shows simulations of a tonically-firing Hodgkin-Huxley model with three conductances with constant injected current (as in Fig. 1). The bottom row shows simulations of a bursting stomatogastric ganglion neuron model with 8 conductances (as in Fig. 5). Ratio of run-time to simulation time (relative speed) as a function of simulation time step (A, B). Simulation error as a function of the step size (C, D). Relative speed of integration as a function of the simulation length (E, F). Relative speed of integration, normalized by system size, as a function of the number of compartments simulated simultaneously (G, H). All benchmarks were performed on the same computer, and all simulators using fixed time-step integration methods. NEURON was run using the Python wrapper.